Spatiotemporal variability and propagation of equatorial noise observed by Cluster

O. Santolík,[1] J. S. Pickett, and D. A. Gurnett
Department of Physics and Astronomy, University of Iowa, Iowa City, Iowa, USA

M. Maksimovic
Laboratoire d'Etudes Spatiales et d'Instrumentation en Astrophysique, Observatoire de Paris-Meudon, Meudon, France

N. Cornilleau-Wehrlin
Centre d'Etude des Environnements Terrestre et Planétaires, Vélizy, France

Received 5 November 2001; revised 20 March 2002; accepted 2 May 2002; published 31 December 2002.

[1] We report a multipoint case study of the electromagnetic equatorial noise observed by the Cluster project. High-resolution data were measured in three close points in space located in the morning sector of the outer plasmasphere. We demonstrate a narrow latitudinal extent of the emissions with a typical width of 2°, centered near the minimum-B equator. Power spectra recorded by the different satellites show a complex structure of emission lines whose relative intensities and positions vary at timescales of 1–2 min and/or at spatial scales of tens of wavelengths. These lines do not match harmonics of the local proton cyclotron frequency, as it would be expected if the waves are generated by energetic ions and observed near the source region. We bring observational evidence that the waves propagate with a significant radial component and thus can propagate from a distant generation region located at different radial distances where ion cyclotron frequencies match the observed fine structure. *INDEX TERMS:* 6939 Radio Science: Magnetospheric physics; 2730 Magnetospheric Physics: Magnetosphere—inner; 2772 Magnetospheric Physics: Plasma waves and instabilities; 2768 Magnetospheric Physics: Plasmasphere; 2794 Magnetospheric Physics: Instruments and techniques; *KEYWORDS:* waves in plasmas, inner magnetosphere, equatorial emissions

Citation: Santolík, O., J. S. Pickett, D. A. Gurnett, M. Maksimovic, and N. Cornilleau-Wehrlin, Spatiotemporal variability and propagation of equatorial noise observed by Cluster, *J. Geophys. Res.*, *107*(A12), 1495, doi:10.1029/2001JA009159, 2002

1. Introduction

[2] Equatorial noise consists of electromagnetic plasma waves propagating in the close vicinity of the geomagnetic equatorial plane at frequencies from a few hertz to several hundreds of hertz. *Russell et al.* [1970] first found these emissions in the outer plasmasphere within ~2° from the equator, at frequencies between twice the local proton cyclotron frequency (f_{H+}) and half the lower hybrid frequency (f_{lh}). They also found that the magnetic field fluctuations are nearly linearly polarized, consistent with propagation in the cold-plasma whistler mode [*Stix*, 1992], and with wave vectors within 1° of perpendicular to the static magnetic field ($\mathbf{B_0}$). *Gurnett* [1976] analyzed equatorial crossings at radial distances (R) from 2 to 3.5 R_E and found that intense noise occurs within 10° from the magnetic equator, but the majority of cases were confined within 5° from the equatorial plane. Wide-band time-frequency spectrograms showed that the noise consists of many spectral lines with different frequency spacings. *Gurnett* [1976] suggested that these lines are created by ion cyclotron harmonic interaction in a region where the local cyclotron frequency matches the observed spacing and that the waves subsequently propagate in the electromagnetic whistler mode to the observation point. *Perraut et al.* [1982] published a statistical study at R = 4 – 8 R_E in the frequency range 0.2–12 Hz. They generally observed this structured noise below 7 R_E and within 10° from the magnetic equator, with the first spectral line around or above the local f_{H+}. On the basis of simultaneous measurements of energetic protons they proposed a wave generation model using ring-like distribution functions at a pitch angle of 90°. *Laakso et al.* [1990] analyzed electric field fluctuations at R = 6.6 R_E and at frequencies below 11 Hz and found that the waves propagate azimuthally, i.e., in the direction perpendicular to the local magnetic meridian plane. *Kasahara et al.* [1994] confirmed these results at frequencies below 80 Hz (i.e., below 3 f_{H+} for R = 2 – 2.5 R_E) and suggested that the waves propagate azimuthally near the plasmapause, trapped by the density gradient.

[3] This paper presents a case analysis of equatorial noise at frequencies above ~9 f_{H+}, simultaneously observed by

[1]Now at Faculty of Mathematics and Physics, Charles University, Prague, and at Institute of Atmospheric Physics, Czech Academy of Sciences, Prague, Czech Republic.

0148-0227/02/2001JA009159$09.00

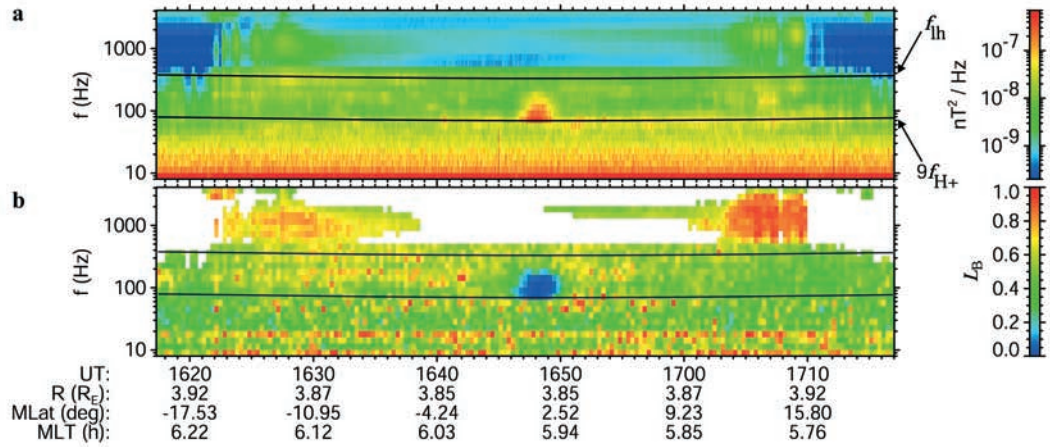

Figure 1. (a) Time-frequency power spectrogram of magnetic field fluctuations recorded by the STAFF-SA instrument on board Cluster 1 on 4 December 2000. (b) Ellipticity obtained as ratio of minor to major axis of the magnetic field polarization ellipse and plotted for intensities larger than 10^{-9} nT^2/Hz. Position is given below the spectrogram: R is radial distance; MLat is magnetic dipole latitude; MLT is magnetic local time. Overplotted lines indicate $9\,f_H^+$ and f_{lh}. The value for f_{lh} is calculated supposing $f_p \gg f_{ce}$.

three Cluster satellites at a radial distance of 4 R_E. We address location of noise with respect to the equatorial plane and the spatiotemporal structure of its frequency spectra. Since a common feature of the equatorial noise is the presence of harmonic lines whose spacings do not match the local f_{H+}, waves have to propagate radially in order to get from the generation region to the point of observation. The basic problem of this hypothesis is that radial propagation has not yet been confirmed by observations. In this paper we show experimental evidence that, indeed, wave propagation directions have a radial component.

2. Spatiotemporal Structure

[4] Figure 1 shows magnetic field data recorded by the spectrum analyzer of the spatio-temporal analysis of field fluctuations (STAFF-SA) instrument [*Cornilleau-Wehrlin et al.*, 1997, 2002] on board Cluster 1, during a perigee pass on 4 December 2000. The spacecraft is located in the morning sector and moves along its orbit from the Southern to the Northern Hemisphere. The perigee at R = 3.84 R_E closely coincides with the intersection of the geomagnetic equatorial plane just after 1646 UT. Between 1622 and 1710 UT the spacecraft is inside the plasmasphere, as indicated by observations of the plasmapause density gradients by the Whisper instrument (P. Canu, private communication, 2001). This is reflected on the STAFF-SA magnetic power spectrogram (Figure 1a) by the presence of whistler mode hiss emissions at frequencies from f_{lh} ($\sim$300–400 Hz) up to the upper limit of the STAFF-SA band at 4 kHz. Analysis of the full vector measurement of magnetic field fluctuations shows that these emissions are elliptically or nearly circularly polarized. It is displayed in Figure 1b. For the hiss above f_{lh} the ellipticity L_B (ratio of the two axes of the polarization ellipse) is generally higher than 0.5. Close to the equator, between 1646 and 1650 UT, the spectrogram shows a noise emission at frequencies 70–200 Hz. In a clear distinction from the hiss, polarization of these waves is very close to linear, with $L_B < 0.1$. This polarization is expected for the whistler mode equatorial noise.

[5] During this orbit, high-resolution electric field waveforms of the Wideband (WBD) instruments [*Gurnett et al.*, 1997] were acquired through the Deep Space Network (DSN) from three of the four Cluster satellites. These data are complementary to the STAFF-SA measurements. While STAFF-SA provides us with polarization measurements, WBD waveforms allow us to investigate the fine time-frequency structure of the wave emissions. Figure 2 shows time-frequency spectrograms calculated from the WBD waveforms. Similarly, as in the STAFF-SA magnetic field data, the electric component of the equatorial noise is observed by WBD at frequencies between 70 and 190 Hz ($9\,f_{H+} - 0.6\,f_{lh}$), during a short time interval of $\sim$4 min, after each of the satellites passes through the geomagnetic equator. At that time, the satellites were separated mainly along $\mathbf{B_0}$, by $\sim$700 km between Cluster 3 and the leading Cluster 1 and by $\sim$360 km between the last Cluster 2 and Cluster 3. The orbital velocity was directed within 12° from parallel to $\mathbf{B_0}$, and the satellites mainly moved northward perpendicular to the equatorial plane by 0.68° of magnetic latitude per minute. Cluster 1 thus intersected the equatorial plane first, followed by Cluster 3 after $\sim$150 s and by Cluster 2 after another $\sim$75 s. The points where the three satellites encountered the equator are radially separated by $\sim$110 km from the innermost Cluster 3 to Cluster 2, and another $\sim$100 km from Cluster 2 to the outermost Cluster 1 (see Figure 3). Azimuthally, these separations are $\sim$200 km from Cluster 2 (which is most shifted toward the night side) to Cluster 1 and another $\sim$60 km from Cluster 1 to the most Sunward Cluster 3.

[6] The waves were observed in a latitudinal interval <3°, and the observed evolution of power-spectral density is well consistent with a Gaussian latitudinal envelope. A fit of a Gaussian function gives a half-width of 0.8° between the point where the intensity is maximum and the point where the power decreases to the 1/*e* level with respect to the maximum. At these scales the approximation of dipole

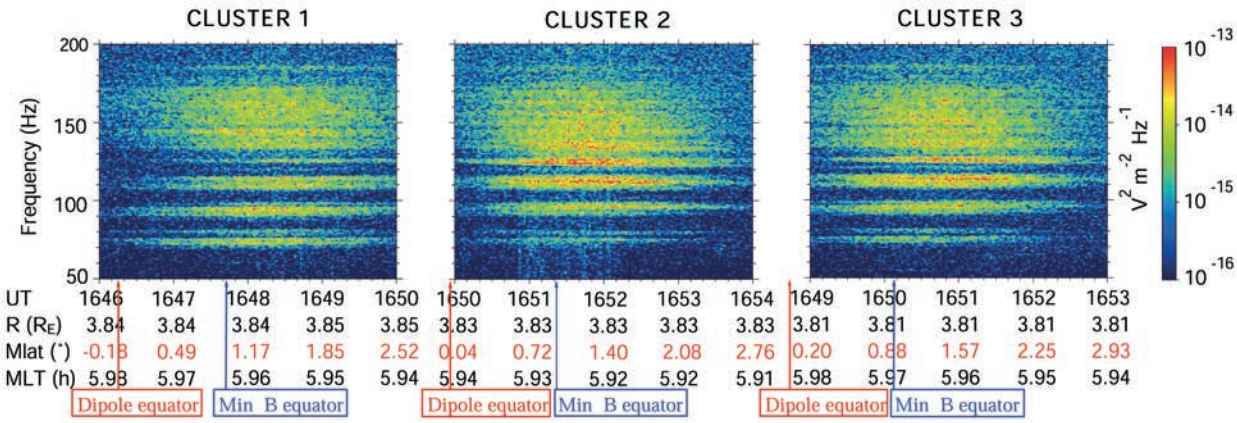

Figure 2. Time-frequency spectrograms of electric field data recorded by the three WBD instruments on 4 December 2000. Common power scale is on the right. Position of the three Cluster satellites is given below the spectrograms, as in Figure 1.

equator becomes insufficient. We have thus determined the magnetic equator by a more appropriate procedure, i.e. by searching for the point where the modulus of $\mathbf{B_0}$ is minimum along a given field line. We have traced model field lines using the Geopack program, involving the IGRF model and the T89c model of the external field [*Tsyganenko*, 1989]. The resulting "minimum-B" equator is ~1° northward from the dipole equator (see Figure 2). The fit of a Gaussian envelope still gives the maximum intensity shifted by ~0.3° northward from the minimum-B equator, possibly owing to differences of our situation from the model. Note that these results are similar for all the three spacecraft, but there are variations (of the order of 0.3°) of the location and latitudinal extent of wave activity at different frequencies.

[7] The fine structure of spectral lines, seen on the spectrograms, is shown in detail on integrated spectra in Figure 4. We use a frequency resolution of 0.2 Hz, and to reduce the statistical error of spectral estimates we average the 4-min time interval for each satellite, leading to an error of ~12% (a little more than one small tick on the vertical axis). Spectra show emission peaks with several different harmonic spacings. At lower frequencies below 130 Hz the power is concentrated to large peaks spaced by 15–20 Hz, some of them being split into several lines with a closer separation. The location of the main peaks is similar for the three spacecraft, but their relative intensities and the ways in which these peaks are split are significantly different. In this lower part of the spectrum it is not possible to clearly identify a harmonic structure. Some of the peaks seem to follow a harmonic pattern (e.g., peaks at 81, 97.2, and 113.4 Hz could correspond to the 5th–7th harmonics of a fundamental frequency of 16.2 Hz; another system could be consistent with the 4th–6th harmonics of 18.8 Hz), but not all the peaks can be explained by similar patterns of three or more harmonics.

[8] In the upper part of the spectrum above 130 Hz the power is distributed more evenly in a large band extending up to 190 Hz. Narrow emission lines spaced by ≈6.5 Hz appear in this band in the Cluster-2 and Cluster-3 spectra. These distinct narrow lines are absent in the Cluster-1 spectrum but a structure of peaks spaced by one-half of that frequency (about 3.2 Hz) can be recognized in the spectra of all three satellites. A closer look indicates that on Cluster 3, frequencies of the narrow lines match the 21st–26th harmonic of 6.56 Hz, and on Cluster 2 the fundamental frequency seems to be slightly lower, ~6.52 Hz. All these possible fundamental frequencies are, however, significantly different from the local f_{H+}, which is ~8 Hz, and neither do they match the cyclotron frequencies of heavier ions. If the waves were originally generated at frequencies close to multiplies of the ion cyclotron frequency in the source, they must propagate from a different radial distance. Waves with a fundamental frequency of more than 8 Hz would only propagate from lower R where f_{H+} is higher: for major peak spacings below 130 Hz this radial distance of the source would be between R ~ 2.9 and R ~ 3.1 (recall that the point of observation is at R = 3.84). Waves with fundamental frequency below ~8 Hz can propagate from higher R where they match with f_{H+} (in that case the source is at R ~ 4.1), but they also can propagate from lower R if

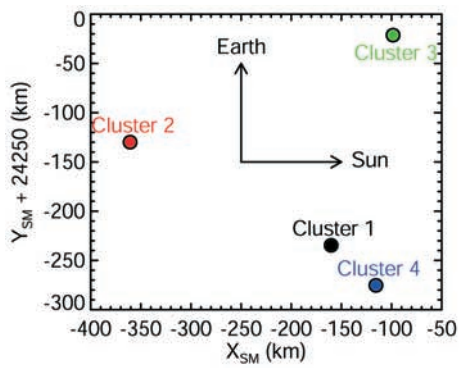

Figure 3. Positions of points where the Cluster satellites encountered the equator near their perigee on 4 December 2000. The positions are given in the Solar-Magnetic (SM) coordinates. Cluster 4 is included, but no WBD data are available from this satellite. Arrows show directions toward the Earth and toward the Sun.

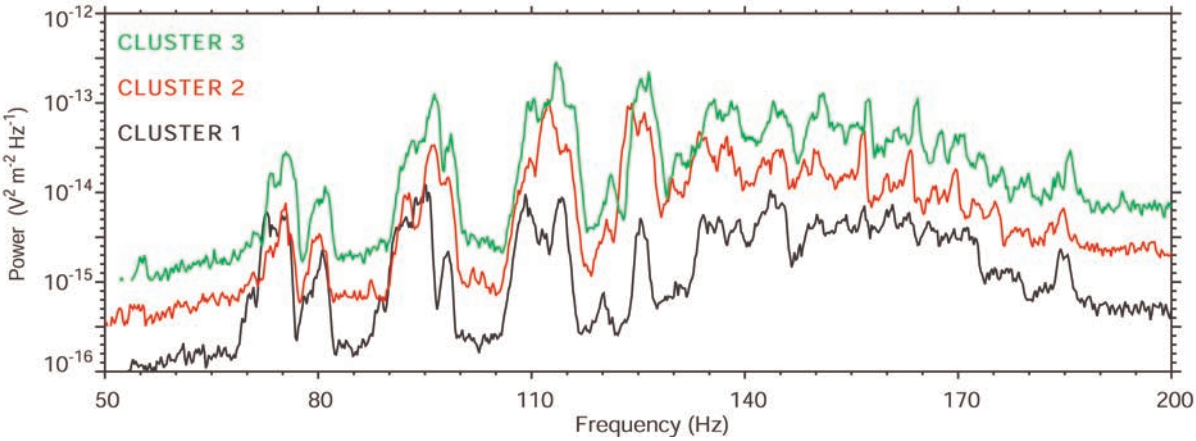

Figure 4. Power spectra integrated during the 4-min intervals shown in Figure 2 for each of the satellites. Vertical scale is drawn for Cluster 1 (black solid line), spectrum from Cluster 2 (red line) is shifted upward by half an order of magnitude, and the spectrum of Cluster 3 (green line) is shifted by an order of magnitude.

they are connected with cyclotron frequencies of heavier ions ($R \sim 2.6$ for He^+).

3. Propagation

[9] Basic propagation properties of equatorial noise have been described by *Russell et al.* [1970], who analyzed magnetic field fluctuations. Using theoretical polarization properties of the whistler mode waves, they found that the wave vectors are nearly perpendicular to $\mathbf{B_0}$, i.e., lie close to the equatorial plane. Assumption that the waves propagate in the whistler mode is supported by both theory and observations. The whistler mode is the only cold-plasma mode existing between the local f_{H+} and f_{lh} and the observed linear polarization of magnetic field fluctuations appears in the cold plasma theory [*Stix*, 1992] for perpendicular wave vectors. Figure 5 shows some wave properties calculated from that theory using parameters adjusted to our experimental situation. We use a two-component plasma model containing cold electrons and cold protons, and the calculations are performed at three wave frequencies covering the interval where we observe the equatorial noise. Two different values of the plasma frequency (f_p) are considered to demonstrate that the ellipticities and the group velocity direction are nearly independent of this parameter, while the wavelength and group velocity modulus scale with its value. Note that the obtained wavelengths are by an order of magnitude lower than the separation of points where the satellites intersected the equatorial plane.

[10] At the lower edge of the observed frequency interval (at a frequency of $9\,f_{H+}$) the predicted ellipticity of magnetic field fluctuations corresponds to the observed values (L_B below 0.1) for wave vectors within 0.8° of perpendicular to $\mathbf{B_0}$. This interval reduces to 0.2° for the highest frequencies where we observe the equatorial noise ($f = 25\,f_{H+}$). For these wave vectors, however, the group velocity is still deviated by only 15–40° from the $\mathbf{B_0}$ direction. Even stronger conditions on perpendicularity of wave vector directions must thus be imposed for waves staying in the equatorial plane during their propagation. These waves also propagate with group velocities of the order of several hundreds of kilometers per second, i.e., by an order of magnitude slower than waves deviated by just 1° of perpendicular to $\mathbf{B_0}$.

[11] For quasi-perpendicular wave vectors the electric field fluctuations are elliptically polarized with a low ellipticity, but their polarization is never exactly linear (L_E ranges from 0.02 to 0.11). For these wave vectors the theory also predicts that the direction of the magnetic field fluctuations is along $\mathbf{B_0}$ and that the major polarization axis of the electric field fluctuations is directed along the wave vector (not shown in Figure 5). Polarization of the magnetic field fluctuations thus cannot be used to find the wave vector direction in the equatorial plane, but from the major polarization axis of electric field fluctuations we can estimate that direction and determine whether the equatorial noise propagates radially. This property was used by *Laakso et al.* [1990] to characterize the wave vector direction in the equatorial plane, and it will also be the basis of our analysis.

[12] Electric field data presented in Figure 4 were measured by 88-m double-probe antennas installed in the spin planes of each of the three satellites. Since these spin planes are within 20° of the magnetic equatorial plane and the electric field is supposed to be elliptically polarized perpendicular to $\mathbf{B_0}$, a spin pattern should appear in the data. Figure 6c shows a waveform captured during a 15-s time interval (several spin periods of ~4 s) near the maximum intensity of equatorial noise on Cluster 1. The signal is passband filtered to the frequency interval 50–200 Hz where the noise is observed. An envelope pulsating with one-half of the spin period is clearly visible on the waveform. Given the elliptic polarization of the electric field, maximum fluctuations are supposed to be seen every time when the antenna most approaches the direction parallel or anti-parallel to the major polarization axis. Since the major polarization axis is parallel to the wave vector, the maximum fluctuations also indicate times when the antenna most approaches the wave vector direction. Times when one tip of the antenna points toward the Sun (blue vertical lines) do not coincide with these maxima nor with the minima but are rather located in between. In this special case, where the

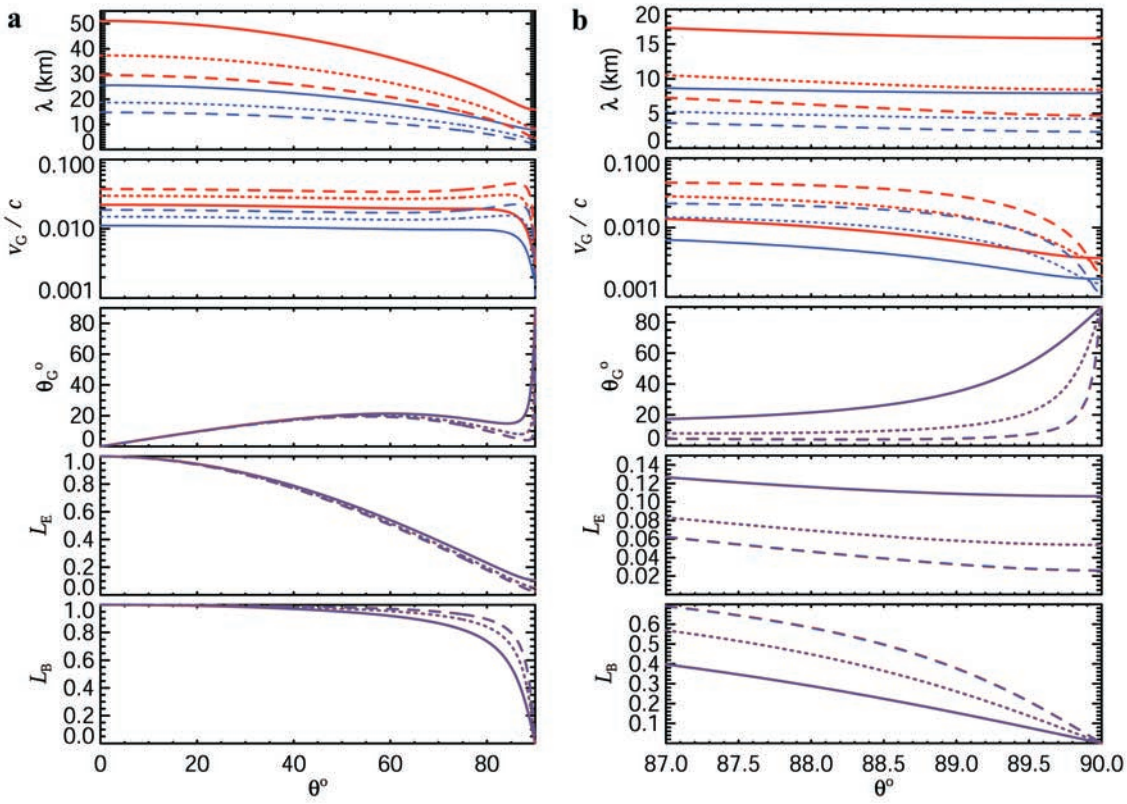

Figure 5. Theoretical properties of whistler mode waves as a function of angle θ between the wave vector and $\mathbf{B_0}$. (a) $0° \le \theta \le 90°$; (b) expanded part $87° \le \theta \le 90°$; (thick red line) $f_p = 6\, f_{ce}$; (thin blue line) $f_p = 12\, f_{ce}$; (solid line) $f = 9\, f_H^+$; (dotted line) $f = 16\, f_H^+$; (dashed line) $f = 25\, f_H^+$; From the top: Wavelength calculated for $f_H^+ = 8$ Hz, group velocity v_G normalized by the speed of light, angle θ_G between the group velocity and $\mathbf{B_0}$, ellipticity L_E of electric field fluctuations, ellipticity L_B of magnetic field fluctuations.

satellite position is very close to 0600 magnetic local time (MLT), maxima directed toward the Sun would mean azimuthal propagation and the maxima in the perpendicular direction would mean radial propagation. The observed waveform rather indicates an oblique propagation with both azimuthal and radial components. However, the accuracy of data timing and antenna directions (a typical uncertainty of spin phase is of the order of 1°) allows us to verify the above indications by a quantitative analysis.

[13] Supposing that the polarization ellipse is contained in the antenna spin plane, we have the power observed by a spinning antenna,

$$S = A_0\left[\cos^2(\phi - \Phi_0) + L_E^2 \sin^2(\phi - \Phi_0)\right], \qquad (1)$$

where A_0 is the maximum power of electric field fluctuations during the spin period, L_E is the ellipticity (ratio of the minor to the major axis) of the polarization ellipse, Φ_0 is angle deviation of the major axis from a fixed direction (we use the direction toward the Sun as a reference), and ϕ is the spin phase with respect to that reference direction,

$$\phi = \frac{2\pi}{T_s}(t - t_0). \qquad (2)$$

Here, T_s is the spin period, t is time, and t_0 is the time when the antenna points toward the reference direction. In equation (1) we assume that the wave frequency is much higher than the spin rate, which condition is well fulfilled in our case. We can thus fit that model to the observed data, taking A_0, Φ_0, and L_E as free parameters. Figure 6a shows power-spectral density of observed electric fluctuations, averaged in the frequency interval 50–200 Hz. Overplotted is the model (equation (1)), found by a nonlinear optimization procedure. This procedure takes into account statistical errors of spectral estimates, $\sigma(S)$ (∼18% in this case, shown by a short vertical line on the top of the figure) and provides us with an estimate of the model parameters and their statistical errors: $A_0 = (4.4 \pm 0.1) \times 10^{-15}\ \mathrm{V^2\,m^{-2}\,Hz^{-1}}$, $\Phi_0 = (46 \pm 1)°$, and $L_E = (0.58 \pm 0.02)$. Note that in addition to these random errors, we must also consider the systematic errors due to the fact that the spin plane is not exactly perpendicular to $\mathbf{B_0}$. This results in underestimation of A_0 by ∼6%, maximum overestimation of Φ_0 by ∼3°, and a maximum possible error of L_E of ∼6%. These errors are close to the random errors of the analysis. Note also that positive Φ_0 is defined in the sense of the satellite spin motion which is opposite to the sense of the Earth's rotation. The major polarization axis is thus located in between azimuthal and radial directions, pointing outward by its Sunward end. That means that the waves travel toward lower R as they propagate from the dayside or toward higher R if they propagate from the nightside. These results clearly show that

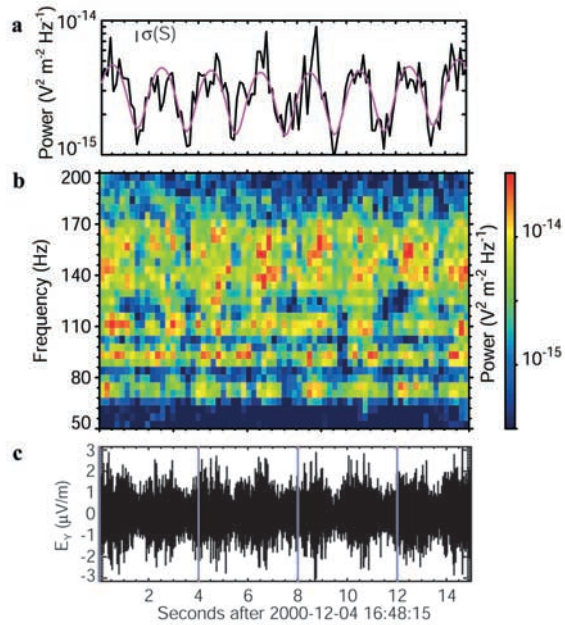

Figure 6. Analysis of a 15-s interval of the electric field data measured by the spinning E_Y antenna on Cluster 1. (a) (thin black line) Average power-spectral density between 50 and 200 Hz and (thick purple line) fit of the spin pattern (see text). (b) Time-frequency spectrogram calculated from this waveform. (c) Waveform filtered between 50 and 200 Hz. Thick vertical lines (blue) indicate times when one tip of the antenna (sphere 3) points toward the Sun.

equatorial noise has a significant radial component which is well beyond experimental uncertainties.

[14] The only problem are the obtained high values of the L_E parameter. For quasi-perpendicular wave vectors expected from the polarization of magnetic field fluctuations, the theory predicts much lower ellipticities of the electric field polarization. Figure 5 gives L_E values between 0.02 and 0.11 in the frequency range considered for the analysis. This would correspond to much deeper spin modulation of wave power than what is actually observed. The spectrogram in Figure 6b shows that although we can often find the basic spin pattern at all frequencies simultaneously, sometimes a substantial part of the power, well above the background level, appears in different spin phases at different times for the different frequencies. This makes questionable the underlying idea of the above procedure, i.e., that there is a single wave vector direction for time periods longer than the analysis interval. To construct a more general model which would better correspond to the data, we have assumed that the power is statistically distributed to wave vectors with a Gaussian probability density in the spin plane. This concept is very similar to the idea of the wave distribution function [*Storey and Lefeuvre*, 1979]. According to the whistler mode theory, we have also supposed that the electric field fluctuations for a given wave vector have a polarization close to linear. The model then reads

$$S = \int_{x_1}^{x_2} A_1 \left\{ \exp\left[-\frac{(x-\Phi_0)^2}{\Delta^2} \right] \cos^2(x-\phi) \right\} dx, \qquad (3)$$

where $x_1 = \Phi_0 - \min(3\Delta, \pi)$, $x_2 = \Phi_0 + \min(3\Delta, \pi)$, A_1 is a normalization parameter, Δ is the angular half-width of the distribution defined by directions where the power distribution falls to $1/e$ of its maximum value at Φ_0, and ϕ is the spin phase defined in equation (2). Nonlinear optimization of the model in equation (3) with free parameters A_1, Φ_0, and Δ leads to S values very close to those obtained from equation (1) and presented in Figure 6a. The Φ_0 parameter is the same for both models, and the depth of the spin pattern modulation now leads to $\Delta = (44.5 \pm 1.1)°$.

[15] Since the frequency spectra observed by the three different satellites are different (Figure 4), the results derived from the spin patterns may also vary. They may also possibly evolve during the passage of each of the satellites through the latitudinal extent of the equatorial noise. We have thus analyzed the spin pattern for the entire time intervals when the equatorial noise was observed by the three Cluster satellites. The signal was divided into subintervals of two spin periods, and the power-spectral density was again averaged in the frequency band 50–200 Hz. In each of the subintervals, parameters of the models in equations (1) and (3) were found by the nonlinear optimization procedure. Figure 7 shows the results versus the magnetic dipole latitude determined from the satellite position in the center of each subinterval. The results for the three satellites are color coded as shown on the top of the figure. Regardless of variations of absolute values of the power-spectral density, the latitudinal evolution of parameter A_0 is the same for the three satellites, and manifests the envelope discussed in Section 2. The evolution of the normalization parameter A_1 is similar, but its interpretation is less obvious because the

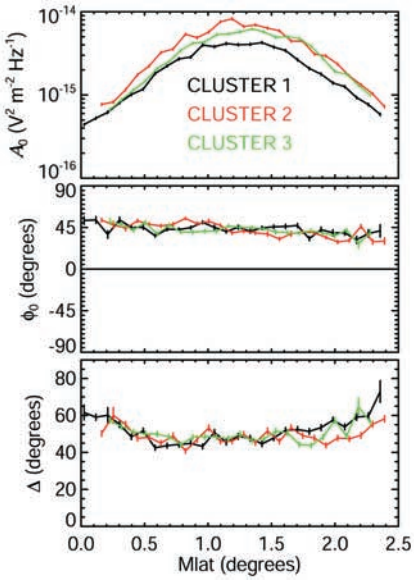

Figure 7. Parameters of the model spin pattern as a function of the magnetic dipole latitude for the three Cluster satellites. A_0 is power-spectral density of electric field fluctuations at maximum; Φ_0 is angle deviation of the direction of the maximum from the direction toward the Sun (positive westward); Δ is angular half-width of the Gaussian distribution of the power-spectral density centered on Φ_0 (see text). Short vertical lines indicate statistical errors of the analysis.

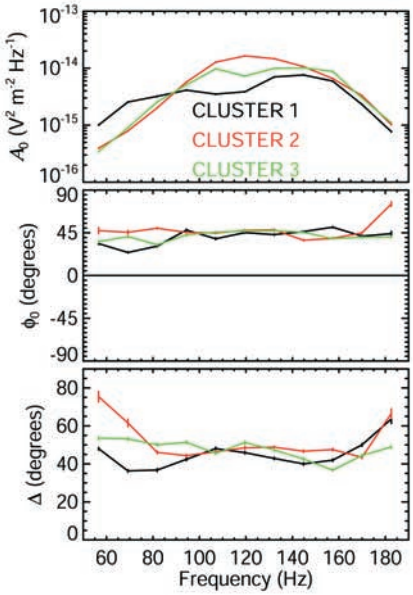

Figure 8. Parameters of the model spin pattern as a function of frequency for the three Cluster satellites. Parameters are the same as in Figure 7.

integration in equation (3) is performed in periodic coordinates. Values of the angle Φ_0 are similar as they were found in the case presented in Figure 6, throughout the entire latitudinal extent of the emission for all the three satellites. The wave vectors where the power is maximum are thus deviated by 25°–55° from the azimuthal direction. Within this interval, there is a slight decreasing trend of average Φ_0 when the satellites move toward higher latitudes. Very similar results as in Figure 6 are also obtained for the angular half-width Δ. For weak wave intensities in the beginning and in the end of the interval, Δ tends to increase, but for more intense waves it fluctuates between 40°–50°. It means that on average, the wave power decreases to $1/e$ of its maximum $\pm(40°–50°)$ from Φ_0, i.e. around the azimuthal or radial directions.

[16] To decrease the statistical errors on spectral estimates, the above analysis was based on data averaged over the entire frequency range of observed equatorial noise. Figure 6 indicates that this does not bias the results because the spin pattern is similar at different frequencies. Figure 8 backs up those indications quantitatively. It shows the same parameters as in Figure 7 but this time as a function of frequency. The results were obtained by optimization of the spin pattern models for a 30-s data interval taken when the maximum intensity was observed on each of the three satellites. Parameter A_0 approximately follows the spectra in Figure 4 but the frequency resolution is much lower (12.6 Hz) because a sufficient number of data points per spin period is needed. Parameters Φ_0 and Δ give approximately the same result over the entire frequency range, the angular half-widths Δ being again larger for weaker signals.

4. Conclusions

[17] Analysis of equatorial noise observed by the Cluster satellites at frequencies between 9 f_{H+} and 0.6 f_{lh} in the morning sector of the outer plasmasphere at R≈4 leads us to the following conclusions:

1. Latitudinal extent of the equatorial noise is well characterized by a Gaussian envelope decreasing to $1/e$ of the maximum power-spectral density at 0.8° on both sides of the maximum. At these scales the approximation of the magnetic dipole equator is not accurate enough to characterize the position of the equatorial noise and the minimum-B equator is much closer to its observed maximum. These observations are repeated without any significant variability as the three satellites subsequently pass through the equatorial plane.

2. Variability is observed in the power spectra obtained from different satellites at timescales of 1–2 min and at spatial scales of tens of wavelengths. Positions and relative intensities of the fine structure of emission lines are different, and these differences exceed statistical errors of spectral estimates. The observed fine structure does not match the harmonics of the local proton cyclotron frequency but can correspond to ion cyclotron frequencies at different radial distances.

3. Propagation directions derived from the observed spin pattern have a significant radial component. The noise thus can propagate from different radial distances. On average the waves propagate at ∼45° between the radial and azimuthal directions, but the wave power is spread in a large angular interval. For radial and azimuthal propagation, the average wave power decreases to $1/e$ of its maximum. These results are very similar for the different satellites, and throughout the latitudinal extent and frequency range of the equatorial noise.

5. Discussion

[18] The observed latitudinal extent of the equatorial noise is lower and the noise is better centered on the equator than an average case from previously published statistical studies [*Gurnett*, 1976; *Perraut et al.*, 1982]. The reason is probably connected to the particular coincidence of the Cluster orbit and dipole tilt which characterizes the presented case. Since the satellites move nearly perpendicular to the equatorial plane, they scan the latitudinal extent of the noise very quickly and at a nearly fixed R and MLT. Such coincidence is rather unlikely within published data, and reported larger latitudinal extents may be due to a combination of temporal or spatial variations during the measurement. Some of the statistical results could also be influenced by the difference between the minimum-B and the dipole equator usually used as a reference.

[19] The most important result of our analysis is the observation of the radial propagation of equatorial noise. All three satellites give very similar results which means that there are no substantial variations of the propagation mode on the timescales of minutes. At timescales of seconds (i.e., less than the spin period) we, however, observe random departures from a regular spin pattern, accounting for a much lower spin modulation than would correspond to a reasonably low ellipticity of electric field fluctuations. In this situation we have no better possibility than to describe the propagation statistically, by a distribution of wave power between different azimuthal wave vector directions. The result indicates that waves can

simultaneously travel on very different paths from a possibly extended generation region to the point of observation. The propagation from the source can be strongly affected by azimuthal and radial variations of the plasma density.

[20] Evidence of harmonic emission lines which are slightly downshifted in frequency on Cluster 2 with respect to the observations on Cluster 3 could provide other indications on the way the waves travel from the source. The two satellites probably observe waves from different localized sources or rather from different regions of the same extended source. Propagation from the source and possibly the generation of the equatorial noise can also be influenced by particular properties of the group velocity at these frequencies. Its direction can be far from the equatorial plane even if the wave vectors are very close to that plane, and it moves toward the equatorial plane only for wave vectors within small fractions of a degree from perpendicular to $\mathbf{B_0}$. The group velocity modulus substantially decreases for these wave vectors. This can influence the time during which a wave packet passes through a generation region.

[21] In the bottom half of the observed spectrum the fine structure of emission lines is rather complex, and it is not easy to clearly identify harmonic series of lines, previously reported by, e.g., *Gurnett* [1976] and *Perraut et al.* [1982]. Especially, if we do not exclude the possibility that some series have less than three harmonics present in the spectra, the peaks can be attributed to several different combinations of series, and we cannot distinguish which of the possible solutions to this problem is more likely. Secondary emission lines found around the large peaks could also account for another possibility, originally suggested by *Perraut et al.* [1982]: some of the lines can possibly be created by a nonlinear interaction between waves at different frequencies. For instance, some close lines can originate from nonlinear modulation of a higher frequency signal by a low frequency component, rather than from the linear superposition of two signals at close frequencies, each of them taking part in another harmonic series with different fundamental frequencies. These possibilities cannot be easily distinguished using the WBD waveforms where the low-frequency signals (<50 Hz) are suppressed by a high-pass filter.

[22] Spectra observed by Cluster 1 show remarkably more differences compared with the other two satellites. There is no substantial difference between separations of points where the satellites cross the equator, all of them are of the order of 200 km. The major difference is that Cluster 1 crosses the equator about twice as earlier (~2.5 min) before Cluster 3 than does Cluster 3 before Cluster 2 (~1.25 min). This seems to suggest that the observed differences are rather temporal than spatial, but inhomogeneities localized in space cannot be excluded. The answer can be given only on the statistical basis. A statistical study involving a large number of multispacecraft observations is needed to better understand these spatiotemporal relations and propagation of equatorial noise from its generation region.

[23] **Acknowledgments.** We thank J. Dowell and R. Brechwald who prepared the preprocessing software for the WBD, R. Huff who made the WBD calibration, and Per-Arne Lindqvist (KTH Stockholm) who provided us with the directions of antennae booms. We acknowledge the access to the spin-resolution data of the FGM magnetic field experiment (PI A. Balogh) used for reference to check the accuracy of the model of the static magnetic field. The WBD instrument was supported by the NASA Goddard Space Flight Center under grant NAG5-9974. O. Santolík thanks the Fulbright commission in Prague for support during his stay in Iowa and acknowledges the support of the Czech Grant Agency grant 205/01/1064.

[24] Lou-Chuang Lee and Chin S. Lee thank Harri E. Laakso and another reviewer for their assistance in evaluating this paper.

References

Cornilleau-Wehrlin, N., et al., The Cluster spatio-temporal analysis of field fluctuations (STAFF) experiment, *Space Sci. Rev.*, *79*, 107–136, 1997.

Cornilleau-Wehrlin, N., et al., First results obtained by the Cluster STAFF experiment, *Ann. Geophys.*, in press, 2002.

Gurnett, D. A., Plasma wave interactions with energetic ions near the magnetic equator, *J. Geophys. Res.*, *81*, 2765–2770, 1976.

Gurnett, D. A., R. L. Huff, and D. L. Kirchner, The wide-band plasma wave investigation, *Space Sci. Rev.*, *79*, 195–208, 1997.

Kasahara, Y., H. Kenmochi, and I. Kimura, Propagation characteristics of the ELF emissions observed by the satellite Akebono in the magnetic equatorial region, *Radio Sci.*, *29*, 751–767, 1994.

Laakso, H., H. Junginger, A. Roux, R. Schmidt, and C. de Villedary, Magnetosonic waves above f_c (H+) at geostationary orbit: GEOS 2 results, *J. Geophys. Res.*, *95*, 10,609–10,621, 1990.

Perraut, S., A. Roux, P. Robert, R. Gendrin, J.-A. Sauvaud, J.-M. Bosqued, G. Kremser, and A. Korth, A systematic study of ULF waves above F_{H+} from GEOS 1 and 2 measurements and their relationships with proton ring distributions, *J. Geophys. Res.*, *87*, 6219–6236, 1982.

Russell, C. T., R. E. Holzer, and E. J. Smith, OGO 3 observations of ELF noise in the magnetosphere, 2, The nature of the equatorial noise, *J. Geophys. Res.*, *73*, 755–768, 1970.

Stix, T. H., *Waves in Plasmas*, Am. Inst. of Phys., New York, 1992.

Storey, L. R. O., and F. Lefeuvre, The analysis of 6-component measurements of a random electromagnetic wave field in a magnetoplasma, 1, The direct problem, *Geophys. J. R. Astron. Soc.*, *56*, 255–270, 1979.

Tsyganenko, N. A., A magnetospheric magnetic field model with a warped tail current sheet, *Planet. Space Sci.*, *37*, 5–20, 1989.

N. Cornilleau-Wehrlin, CETP, 10/12 Avenue de L'Europe, F-78140 Velizy, France. (nicole.cornilleau@cetp.ipsl.fr)

D. A. Gurnett and J. S. Pickett, Department of Physics and Astronomy, University of Iowa, Iowa City, IA 52242-1479, USA. (gurnett@space.physics.uiowa.edu; jsp@space.physics.uiowa.edu)

M. Maksimovic, LESIA, Observatoire de Paris-Meudon, Place Jules Janssen, F-92195 Meudon Principal Cedex, France. (milan.maksimovic@obspm.fr)

O. Santolík, Faculty of Mathematics and Physics, Charles University, V Holešovičkách 2, CZ-18000 Praha 8, Czech Republic. (ondrej.santolik@mff.cuni.cz)